Applied Catalysis B: Environmental 91 (2009) 269–274

Contents lists available at ScienceDirect

Applied Catalysis B: Environmental

journal homepage: www.elsevier.com/locate/apcatb

Study of different bimetallic anodic catalysts supported on carbon for a high temperature polybenzimidazole-based direct ethanol fuel cell

Justo Lobato *, Pablo Cañizares, M.A. Rodrigo, Jose J. Linares

Chemical Engineering Department, University of Castilla La-Mancha, Enrique Costa Building, Camilo José Cela Avenue, 12, 13071 Ciudad Real, Spain

ARTICLE INFO

Article history:
Received 26 March 2009
Received in revised form 20 May 2009
Accepted 23 May 2009
Available online 6 June 2009

Keywords:
DEFC
High temperature
Polibenzimidazole membrane
Pt–Ru/C
Pt–Sn/C

ABSTRACT

In this work, two different catalysts, Pt–Ru (1:1), Pt–Sn (1:1), supported on both non-activated and activated carbon for the electro-oxidation of ethanol were studied in a H_3PO_4 doped polybenzimidazole-based fuel cell, using vapor fed ethanol and operating in the range of 150–200 °C. The catalysts were synthesized using $NaBH_4$ as reducing agent and were characterized by X-ray diffraction, inductively coupled plasma-atomic emission spectroscopy and temperature programmed reduction. The best performance was reached at the highest temperature and with the catalyst based on Pt–Ru/C_{act}, using activated carbon as support. The best results for the Ru-based catalyst can be explained by the higher level of alloying reached for the Ru than that for Sn, which modifies the crystalline structure of Pt and enhances the activity oxidation of ethanol and of intermediates that can be generated during the oxidation of ethanol.

1. Introduction

Ethanol is less toxic and less volatile than methanol. It can be produced by fermentation of sugar-containing biomass resources, and is then renewable in nature. Moreover, it has high energy density. As a liquid fuel, ethanol also avoids issues of storage that appears for hydrogen systems. A fuel cell able to direct oxidation of ethanol to carbon dioxide and water will produce 12 electrons and it will be a potentially attractive energy resource. However, in all the fields of alcohol-based solid polymer electrolyte fuel cells, some issues still need to be overcome: the sluggish kinetic of the alcohol electro-oxidation process, and the fuel crossover, which depolarizes the cathode and reduces the efficiency of the system [1,2]. One alternative to sort out these problems is to increase the operating temperature above 100 °C, enhancing the kinetic of the ethanol oxidation [3]. Along with this, if a membrane with low fuel permeability was used, the scenario would be ideal. A possible candidate that can fulfil all the prerequisites previously mentioned is H_3PO_4 doped polybenzimidazole (PBI) [4,5]. Proton exchange membrane fuel cell (PEMFC) operating at high temperatures has in recent years been recognized as a promising solution to meet the different technical challenges of fuel cell systems [6]. In the review by Li et al. [6] it can be found that PBI can suit all the applications and not only for hydrogen as fuel, but also for methanol [7–9] and ethanol [4,10] as fuel.

The electro-oxidative removal of CO-like intermediates and the cleavage of C–C bond are the two main obstacles and rate-determining steps. The ethanol electrochemical reaction activity can be enhanced not only by increasing temperature but also by using high active electrocatalysts [11]. There is a long list of catalysts that have demonstrated the faculty to electrochemically oxidize small alcohols. The more extensively researched anode catalyst for direct methanol and ethanol fuel cells are the binary Pt–Ru and Pt–Sn and the correlated ternary catalysts [1]. All of them have been used at low temperature conditions, maximum 130 °C with Nafion membranes as electrolyte [2,11,12]. To increase their electrochemically active surface area, metal catalysts are supported on high surface area materials, commonly carbons. Carbon blacks are widely used as catalyst support in low temperature fuel cells due to its low cost and high availability [13]. Ethanol electro-oxidation involves more intermediates and products than that of methanol, and then more active electrocatalysts are required to promote ethanol electro-oxidation. The nature and structure of the electrocatalysts play a crucial role in ethanol adsorption and electro-oxidation, and the catalyst preparation procedure affects the catalysts nature and structure, especially the various interactions between the different elements [11].

Taking into account all these items, the present work shows the performance of a direct ethanol fuel cell, fed as vapor in a high temperature PEMFC using phosphoric acid doped PBI as electrolyte. The effect of the carbon support (activated and non-activated carbon) on the direct ethanol fuel cell (DEFC) performance has been analyzed using different anodic catalyst prepared in our lab,

* Corresponding author. Tel.: +34 926 295 300; fax: +34 926 295 256.
E-mail address: justo.lobato@uclm.es (J. Lobato).

0926-3373/$ – see front matter © 2009 Elsevier B.V. All rights reserved.
doi:10.1016/j.apcatb.2009.05.035

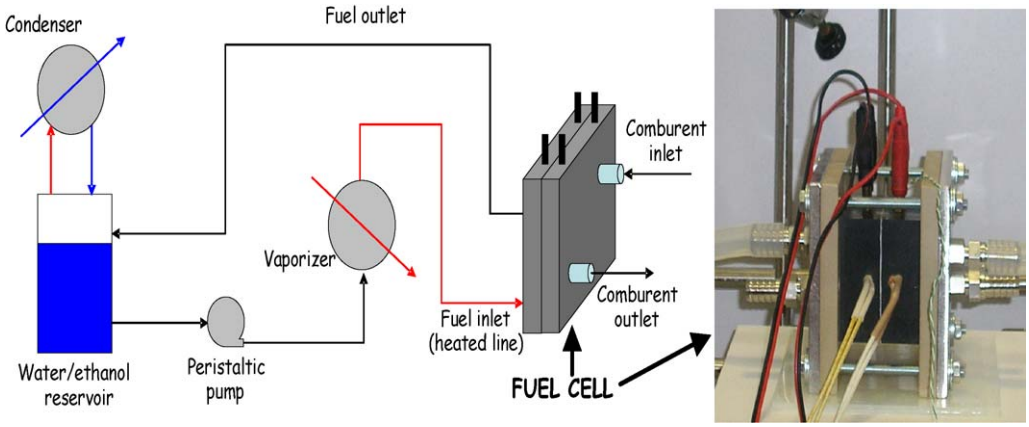

Fig. 1. Scheme of the experimental setup and a picture of the fuel cell.

bimetallic catalysts supported on a commercial carbon black (Pt–Ru/C, Pt–Sn/C) when the cell was run at high temperature (150–200 °C).

2. Experimental

2.1. Preparation of catalyst

Among the different methods that can be used to synthesize bimetallic Pt-based electrocatalysts for fuel cell applications, the impregnation method is most widely used because the process is simple. This method includes many variables, such as the use of different reducing agent and metal precursors, different means of mixing the reducing agent and changing the pH, which affects the particle size, dispersion, morphology, surface composition, and degree of alloying [14]. In this work, Vulcan XC-72 was used as the carbon support. $H_2PtCl_6{\cdot}6H_2O$, $Cl_4Sn{\cdot}5H_2O$, and Cl_3RuxH_2O (38%) were used as precursors of the catalysts. The amount of metal precursors was adjusted so that both Pt and Ru and Pt and Sn had a molar ratio of 1:1. The total metal content in the catalyst was 60%. The mixture of the precursors and carbon in water and acetic acid (humidifying agent) was vigorously stirred and heated up to 80 °C. Once it reached 80 °C, 20 ml of $NaBH_4$/g of metal was added to the mixture as reducing agent. Then, the mixture was filter and washed with heated water at 80 °C three times and finally the catalysts were dried in a vacuum oven at 100 °C for 4 h.

In order to prepare catalyst supported on activated carbon, the Vulcan XC-72 was treated as follows: 35 ml HCl/g carbon was added to ground carbon and heated at 120 °C for 10 h under total reflux conditions. After cooling to room temperature, the mixture was filtered, washed, and dried in an oven for one night (12 h). 25 ml HNO_3/g solid was added to the ground solid and heated at 120 °C for 10 h under total reflux conditions again. Finally, after cooling, filtering, and the washing steps, the solid was dried in an oven at 150 °C for 12 h.

XRD patterns were recorded with a Philips X-Ray diffractometer using Cu Kα radiation with a Ni filter. The 2θ angular regions between 20° and 90° were explored at a scan rate of 5°/min. TPR analyses were carried out on Autochem 2950 HP (Micromeritis). The as prepared catalysts were placed in a U-shaped tube and were heated at 5 °C/min under 17 vol.% H_2/Ar. The synthesized catalyst were analyzed by ICP-AE spectroscopy to measure the molar ratio of the metal in the catalysts.

2.2. Electrochemical measurements

On top of a teflonized carbon paper (Toray Graphite Paper, TGPG-120, 0.35 mm thick, 40% PTFE, USA), a catalytic ink was sprayed with the aid of an aerograph (Airnex mod. 300, Spain). For the anode, the metal loading was 4 mg cm^{-2}, PBI (from a solution of 5% PBI in N,N′-dimethylacetamide, DMAc) and the own DMAc as solvent. For the cathode, the catalyst loads were the same except that the catalyst was a commercial one, 60% Pt on Vulcan XC-72 carbon (ETEK-Inc., USA). Once the catalytic layer was deposited, the electrodes were cured at 190 °C for 2 h. Afterwards, these were impregnated with 10% H_3PO_4 in an amount of 6 mol H_3PO_4/mol of polymer and left to soak for 1 day. In order to prepare the assembly, a piece of membrane fabricated in our lab was taken out from the H_3PO_4 doping bath (75% acid), and placed between the electrodes [15,16]. Hot pressing was carried out with the aid of a press, applying a load of 1 tonne and 130 °C for 15 min.

The measurements were carried out galvanostatically from the open circuit voltage (OCV) to higher currents in a 4.65 cm^2 active area fuel cell. The ethanol concentration was 6.7 M (this concentration corresponds to an ethanol water weight ratio of 0.5 and it was selected according to previous results [9]). The collection of the data was carried out waiting until a stable potential was recorded at least for 5 min. Three similar polarization curves were necessary in order to consider stable the response of the system. The anodic polarization curves were recorded by simply flowing N_2 through the cathode, where hydrogen evolution will take place now, turning into a dynamic hydrogen electrode (DHE).

A schematic diagram of the experimental setup is shown in Fig. 1. It consists of a peristaltic pump (Percom-I, JP Selecta, Spain) to impel the liquid mixture, and a vaporizer, consisting of a 2 cm stainless steel pipe wrapped with a heating cable. The fuel exhaust leaves the cell to a condenser, a glass coil (Mervilab, Spain) cooled down with water. The condensate is returned to the feed reservoir (1500 ml), permitting to operate the cell for many hours on a single solution. Every 2 or 3 days the fuel was restored. The used flows were 500 ml min^{-1} for oxygen and 2 ml min^{-1} on a liquid basis (this flow allowed us to vaporize all the liquid and was high enough to avoid mass transfer limitations). A picture of the cell plates is also shown in Fig. 1.

3. Results and discussion

Fig. 2 shows the XRD patterns of the catalysts prepared in our lab. The XRD patterns were very similar when activated carbon was used.

In all catalysts, the peaks assigned to Pt(1 1 1), Pt(2 0 0), Pt(2 2 0), and Pt(3 1 1) planes were observed. In the case of catalysts that contain Sn, the presence of SnO_2(1 1 0), SnO_2(1 0 1), and SnO_2(2 1 1) was observed. Pt lattice parameters of these carbon-supported catalysts were calculated from the (2 2 0)

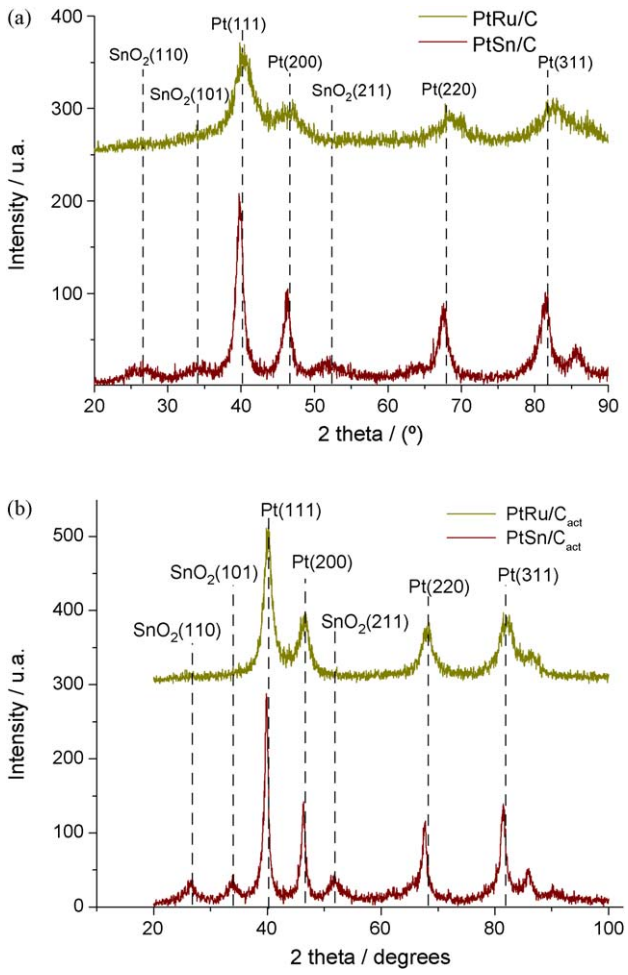

Fig. 2. XRD patterns of the catalysts prepared in the lab (A) with non-activated carbon; (B) with activated carbon.

diffractions peak position in the XRD pattern and shown in Table 1. Moreover, the crystallite size according to the Scherrer equation, the Ru or Sn atomic fractions in the alloy, assuming the Vegard's law [17,18] are given in Table 1.

From Table 1, the lattice parameters of Sn-based bimetallic catalyst are larger than those of pure Pt/C and smaller than those of Pt_3Sn/C [17]. It can be observed that the amount of Sn alloyed with Pt metal is very small. This was corroborated by the presence of SnO_2 in the XRD and TPR profiles as it will be observed later in Fig. 4. The lattice parameter of Pt/C catalyst is 0.3913 [18]. Taking into account the different atomic sizes (R_{Pt} = 0.139 nm, R_{Ru} = 0.134 nm and R_{Sn} = 0.161 nm) the addition of Sn or Ru had a different effect on the crystal structure of Pt/C catalyst [18]. Thus, the inclusion of the smaller atomic size Ru results in the contraction of Pt lattice parameter, as it can be seen in Table 1. Moreover, the atomic content of alloyed Ru was 0.26 and 0.24 for carbon and activated carbon, respectively, which means that only 50% is alloyed with Pt metal. In the case of Sn (bigger atomic radius than Pt metal), is not practically alloyed with Pt, since the values of the lattice parameter are very close to the Pt/C one. This means that Sn is not integrated into the crystalline structure of the Pt and is forming different oxides, as it was observed by the XRD analysis. With respect to the crystallite size, a very high value (it was measure three times) for the $Pt–Sn/C_{act}$ can be observed that could be due to a certain agglomeration phenomenon. In the case of Ru-based catalyst, the crystal size is higher for the activated carbon. This may be due to a lower alloying level that means a lower contraction of the crystal. The obtained bulk atomic ratios of the catalysts from ICP-AES showed that the atomic ratio was the expected 1:1 (error minor than 6%) for all catalysts prepared.

Table 1
Data obtained from XRD analysis.

Catalyst	Lattice parameter (nm)	Crystallite size (nm)	Ru or Sn atomic fraction in the alloy
Pt–Ru/C	0.3876	3.04	0.26
Pt–Sn/C	0.3917	2.78	0.025
$Pt–Ru/C_{act}$	0.3879	3.58	0.24
$Pt–Sn/C_{act}$	0.3918	6.25	0.028

Fig. 3 shows the TPR profiles of the bimetallic catalysts supported on both non-activated and activated carbon. In the case of Pt–Ru catalysts, the peaks at around 320–350 °C and 550 °C approx. are assigned to the reduction of RuO_x to Ru, and of PtO_y to Pt, respectively. The carboxylic oxides on the surface of Vulcan XC-72 begin to be reduced at about 420 °C [19]. Moreover, the desorption area of the catalyst could characterize the amount of Pt unalloyed with Ru. Small one indicates high alloying degree, whereas large one represents low alloying degree. When Pt and Ru form alloy, there is only one reduction peak between 300 °C and 500 °C for commercial Pt–Ru black [19]. Taking into account all of this, it can be observed that, in our case, not all Pt and Ru are forming an alloy. Furthermore, according to the desorption areas it can be said that alloying degree of $Pt–Ru/C_{act}$ is lower than that of Pt–Ru/C, which is in agreement with the XRD results.

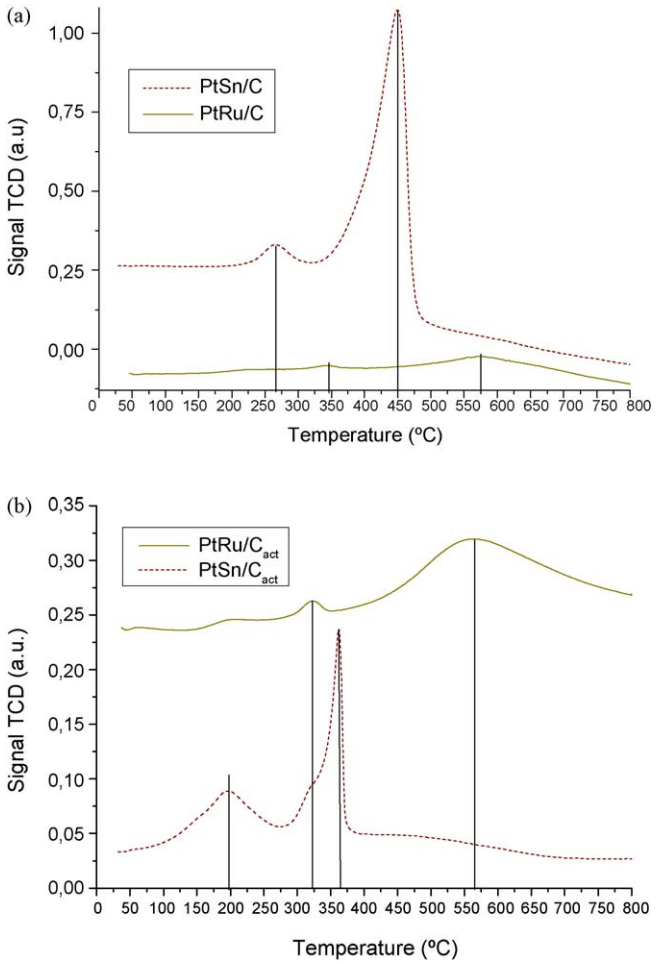

Fig. 3. TPR profiles of the different catalysts prepared under flowing gas of 17 vol.% H_2/Ar. Heating rate: 10 °C/min.

In the case of Sn-based catalyst higher desorption peaks can be observed which means higher amount of oxidized species and then lower alloying levels formed. From Fig. 3 two peaks for the catalysts Pt–Sn/C at 270 °C and 450 °C can be seen, which are attributed to the reduction of surface platinum oxide and SnO, respectively [20–22]. For the Pt–Sn/C_{act} catalyst, the same two peaks but shift to lower temperatures were observed. According to Jiang et al. [21], the reduction peak of SnO_2 occurs at 500 °C approx. Moreover, the reduction temperature of Sn oxide is different and depends on the Pt/Sn ratio, the post-treatment of the synthesized samples and different conditions of hydrogen reduction [22]. Therefore, the big peak that appears between 350 °C and 500 °C could be due to the reduction of both oxides SnO and SnO_2. This fact is easier to observe when the activated carbon was used, where it seems that there are two peaks between 300 °C and 380 °C. What is sure is that Sn is not alloyed very much with the Pt which is in agreement with XRD analysis.

Fig. 4 shows, as an example, the polarization curves and the anodic curves for the Pt–Ru/C catalyst at different temperatures. The positive effect of temperature can be observed, the higher the temperature, the better the cell performs. This is due to the enhancement of the ethanol oxidation kinetics [23]. Moreover, there is another favourable factor, the increase of the PBI conductivity with the temperature [4,5,16]. The anodic curves show that the controlling reaction of the fuel cell is the ethanol oxidation instead of the oxygen reduction, since the polarization curves and the anodic ones are mirror-like images. Moreover, the anodic curves show how the overpotential diminishes with temperature, demonstrating the beneficial effect of an increase in the temperature on the anode kinetic. The same trend was observed for the rest of the catalysts.

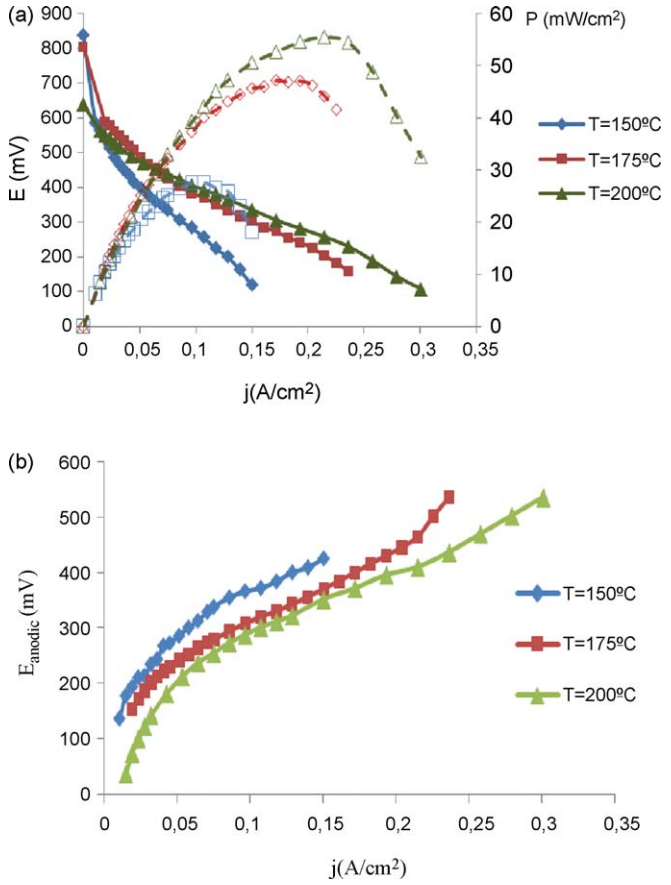

Fig. 4. Performance of Pt–Ru/C catalyst at different temperatures. (A) Polarization curves and power densities. (B) Anodic curves.

In order to compare the performance of the different catalysts, Fig. 5 shows the polarization curves of the catalysts on non-activated carbon at different temperatures. In all cases, the beneficial effect of the temperature on the performance of the fuel cell was observed. Although, it has been reported that Pt–Sn/C

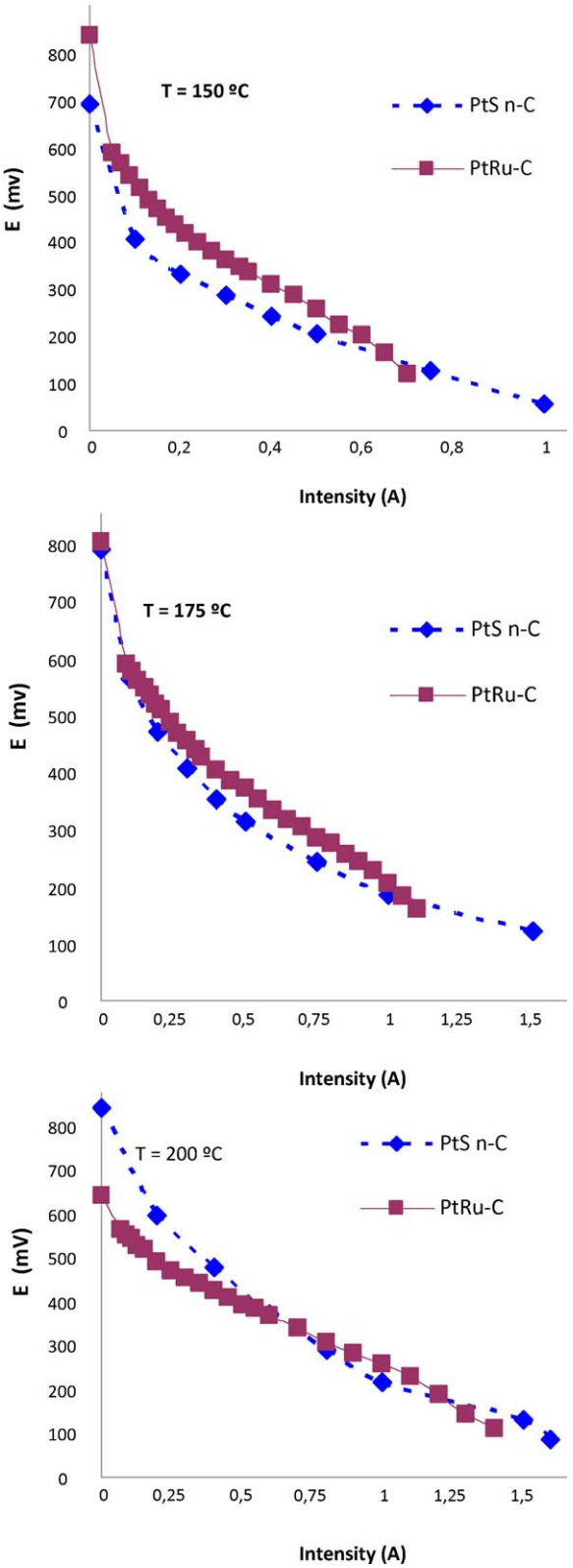

Fig. 5. Polarization curves at different temperatures obtained for the two catalysts prepared with non-active carbon.

catalysts show higher electrocatalytic activity for ethanol oxidation than Pt/C and other binary catalyst [1], compounds with C–C bonds still exist. In our case, at the highest temperature the best performance was achieved by the Pt–Ru catalyst, followed by the Pt–Sn/C one. It must be taken into account, that the oxidation of ethanol is favoured by oxidative species close to Pt sites, which is easier if the secondary metal is present in the crystalline lattice. Thus, these results could be due to the higher level of alloy reached by the Ru with respect to Sn, which would produce a higher amount of oxidative species close to crystalline structure of Pt. In other words, the low alloy level reached for the Pt–Sn/C catalyst could be the main reason that did not allow us to achieve similar results reported by other researchers [1,11,24,25]. So, another catalyst preparation method or another reducing agent is recommendable to prepare Pt–Sn/C catalyst with high levels of alloy that could give higher catalytic activity for the ethanol oxidation.

On the other hand, it is remarkable that as temperature increases the performance gap between the two bimetallic catalyst decreases, reaching the highest open circuit voltage (OCV) at 200 °C in the case of Pt–Sn/C catalyst. This could explain why at high temperature and low current densities (high voltages) the tin oxide species present in our catalyst could be effective for the oxidation of ethanol or intermediate species that are formed during the oxidation of ethanol (acetaldehyde and acetic acid, mainly). Rosseau et al. found that the addition of tin to platinum not only increases the activity of the catalyst towards the oxidation of ethanol and therefore the electrical performance, but also changes the product distribution [26].

With the aim of increasing the ethanol oxidation and then the electrical performance in a fuel cell, the carbon support was activated by mean of the above mentioned acid treatment. Fig. 6 shows the polarization curves at different temperatures for the catalyst synthesized with activated carbon. As it can be seen, the performance expectedly, increases with temperature. In all cases, the best performance was reached for the Pt–Ru/C_{act} (not only the power densities, which increased from 21.3 mW/cm^2 at 150 °C to 79.4 mW/cm^2 at 200 °C but also the OCVs). This behaviour can be explained by the same statement addressed in the case of catalyst supported on carbon. When activated carbon was used, only the Ru metal was able to be alloyed with Pt, as it can be observed in Table 1.

With the aim of comparing the obtained results for all the catalysts studied in this work, Table 2 collects the open circuit voltage (OCV) and maximum power densities for the three temperatures studied and under our experimental conditions. If the effect of the carbon support is compared, the effect is not clear. In the case of Ru it seems that the activation of carbon is positive (at 200 °C, 55.5 mW/cm^2 was obtained for the Pt–Ru/C and 79.4 mW/cm^2 for Pt–Ru/C_{act}) whereas for Sn-based catalyst the effect is negative (as an example, at 200 °C, 49.7 mW/cm^2 was obtained for the Pt–Sn/C and 39.0 mW/cm^2 for Pt–Ru/C_{act}). Li et al. [18] studied the behaviour of Pt–Ru and Pt–Sn supported on a carbon pre-treated with HCl and HNO_3, similar to our procedure but the catalyst were synthesized by a modified polyol method. They obtained similar power densities 45 mW/cm^2 and 55 mW/cm^2 for Pt–Sn and Pt–Ru, respectively, at 90 °C, 2 bar pressure on cathode, 2 mg/cm^2 metal loading on anode and 1 mg Pt/cm^2 on cathode. Generally speaking, the OCV of a DEFC with respect to temperature shows the benefits of elevated temperature [27].

Table 2
OCV and power peak values obtained for the different catalyst studied in this work under our experimental conditions.

Catalyst	Parameter	150 °C	175 °C	200 °C
Pt–Ru/C	OCV (mV)	838	805	638
	Pow_{max} (mW/cm^2)	27.6	47.1	55.5
Pt–Ru/C_{act}	OCV (mV)	588	696	733
	Pow_{max} (mW/cm^2)	21.3	48.2	79.4
Pt–Sn/C	OCV (mV)	693	790	840
	Pow_{max} (mW/cm^2)	22.0	39.8	49.7
Pt–Sn/C_{act}	OCV (mV)	408	466	540
	Pow_{max} (mW/cm^2)	14.6	26.7	39.0

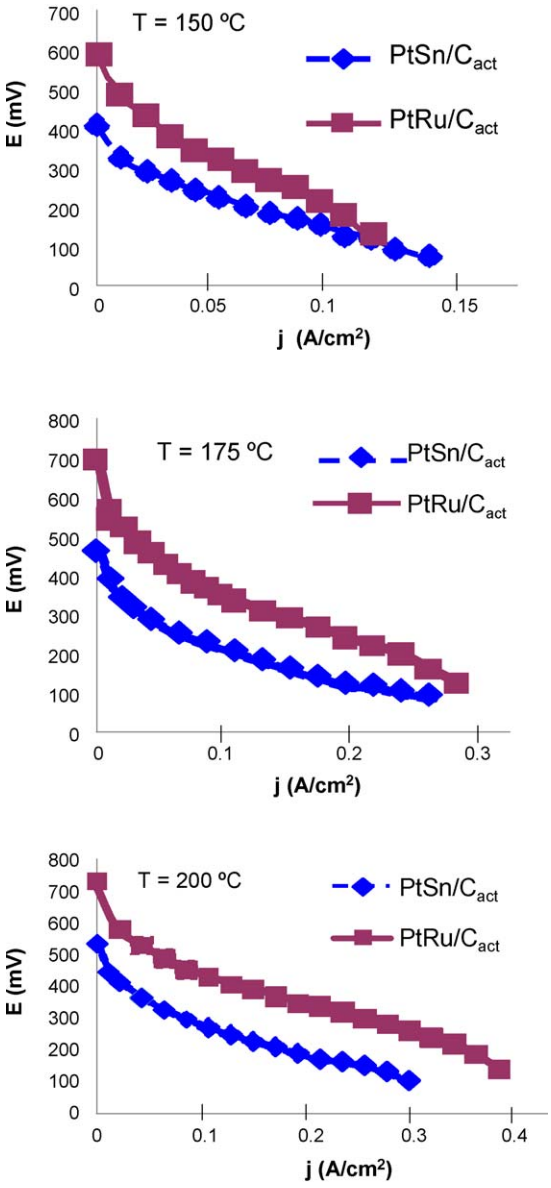

Fig. 6. Polarization curves at different temperatures obtained for the two catalysts prepared with activated carbon.

For supported metal catalyst, the interaction between the metal particle and the support is of great importance to the electrochemical stability. Prado-Burguete et al. [28] found that the resistance to sintering is a function of the number of oxygen surface groups of the support. It was found that the ease of migration of Pt particles is significantly less for carbon containing oxygen surface groups, and the interaction between the metal and support is important in restricting the migration of Pt particles and hence hindering the sintering process. This fact

could explain why at the highest temperature, where the sintering effect is more noticeable, the catalyst Pt–Ru/C_{act} reached the best results which means that they had a better resistance to high temperatures. For the case of Sn-based catalyst, due to the very low alloy level reached, the positive effect of activated carbon is hidden because the Sn particles could occupy the oxygen groups and then the resistance to sintering was not increased.

In a previous work [5], power density values close to 80 mW/cm^2 were reached for the same DEFC under the same conditions but with a commercial Pt–Ru/C and with a Pt loading on anode of 2 mg/cm^2, lower than in the present work. If we take into account that high loading of anode electrocatalysts does not favour the cell performance [29] it can be said that the result obtained with the Pt–Ru/C synthesized in our lab is very satisfactory. However, it can be said, that the synthesis route used is not very advisable in the case of Pt–Sn. A possible explanation for these results is the rapid reducing process of the $NaBH_4$ which makes difficult the alloying of Sn with the Pt and other reducing agent could be more suitable, such as acid formic or ethylene glycol [30]. More work focussing on catalysts supported on carbon, high temperature PEMFC using ethanol as fuel and the analysis of products is under progress in our group.

4. Conclusion

It can be concluded that the Sn-based catalyst was not alloyed with the Pt under the conditions of the synthesis procedure. Only Pt–Ru catalysts were alloyed and only 50% approx.

The best performance of the PBI-based high temperature PEMFC was reached by the Ru-based catalysts under the conditions used in this work. In the case of Ru, the activated carbon had a positive effect and enhanced the performance of the fuel cell, obtaining power densities similar to others obtained with a commercial Pt–Ru/C catalyst. This result confirms that the carbon support has a great importance on the electrochemical activity of the catalysts.

Thus, the PBI-based high temperature PEMFCs are good candidates to be used with direct ethanol fuel because of the high performance due to high temperatures.

Acknowledgments

Authors want to thank the Junta de Comunidades de Castilla-La Mancha (JCCM) and the Company CLM-H2 for the financial support through the Project PBI08-151-2045.

References

[1] E. Antolini, J. Power Sources 70 (2007) 1–12.
[2] M.Y. Wang, J.H. Chen, Z. Fan, H. Tang, G.H. Deng, D.L. He, Y.F. Kuang, Carbon 42 (2004) 3257–3260.
[3] S. Song, Y. Wang, P. Shen, Chin. J. Catal. 28 (2007) 752–754.
[4] J.-T. Wang, S. Wasmus, R.F. Savinell, J. Electrochem. Soc. 142 (1995) 4218–4224.
[5] J. Lobato, P. Cañizares, M.A. Rodrigo, J.J. Linares, Fuel Cells, 2009, in press.
[6] Q. Li, J.O. Jensen, R.F. Savinel, N.J. Bjerrum, Prog. Polym. Sci. 34 (2009) 449–477.
[7] J.S. Wainright, J.-T. Wang, D. Weng, R.F. Savinell, M.J. Litt, Electrochem. Soc. 142 (1995) L121–L123.
[8] J.T. Wang, J.S. Wainright, R.F. Savinell, M. Litt, J. Appl. Electrochem. 26 (1996) 751–756.
[9] J. Lobato, M.A. Rodrigo, P. Cañizares, J.J. Linares, R. López-Vizcaíno, Energy Fuels 22 (2008) 3335–3345.
[10] H. Hou, G. Sun, R. He, Z. Wu, B. Sun, J. Power Sources 182 (2008) 95–99.
[11] W.J. Zhou, W.Z. Li, S.Q. Song, L.H. Jiang, G.Q. Sun, Q. Xin, K. Poulianitis, S. Kontou, P. Tsiakaras, J. Power Sources 131 (2004) 217–223.
[12] C. Lamy, S. Rousseau, E.M. Belgsir, C. Coutanceau, J.M. Leger, Electrochim. Acta 49 (2004) 3901–3908.
[13] E. Antolini, Appl. Catal. B 1 (2009) 1–24.
[14] M.S. Hyun, S.K. Kim, B. Lee, D. Peck, Y. Shul, D. Jung, Catal. Today 132 (2008) 138–145.
[15] J. Lobato, P. Cañizares, M.A. Rodrigo, J.J. Linares, G. Manjavacas, J. Membr. Sci. 280 (2006) 351–362.
[16] J. Lobato, M.A. Rodrigo, P. Cañizares, J.J. Linares, J.A. Aguilar, J. Membr. Sci. 306 (2007) 47–55.
[17] E. Antolini, F. Colmati, E.R. González, Electrochem. Commun. 9 (2007) 398–404.
[18] H. Li, G. Sun, L. Cao, L. Jiang, Q. Xin, Electrochim. Acta 52 (2007) 6622–6629.
[19] J. Guo, G. Sun, S. Sun, S. Yan, W. Yang, J. Qi, Y. Yan, Q. Xin, J. Power Sources 168 (2007) 299–306.
[20] G. Baronetti, S. de Miguel, O. Scelza, A. Castro, Appl. Catal. 24 (1986) 109–116.
[21] L. Jiang, G. Sun, Z. Zhou, W. Zhou, Q. Xin, Catal. Today 93–95 (2004) 665–670.
[22] Y. Guo, Y. Zheng, M. Huang, Electrochim. Acta 53 (2008) 3102–3108.
[23] S. Song, W. Zhou, J. Tian, R. Cai, G. Xin, S. Kontou, P. Tsiakaras, J. Power Sources 145 (2005) 266–271.
[24] A.O. Neto, R.R. Dias, M.M. Tusi, M. Linardi, E.V. Spinacé, J. Power Sources 166 (2007) 87–91.
[25] W. Zhou, Z. Zhou, S. Song, W. Li, G. Sun, P. Tsiakaras, Q. Xin, Appl. Catal. B: Environ. 46 (2003) 273–285.
[26] S. Rousseau, C. Coutanceau, C. Lamy, J.-M. Leger, J. Power Sources 158 (2006) 18–24.
[27] S. Basu, A. Agarwal, H. Pramanik, Electrochem. Commun. 10 (2008) 1254–1257.
[28] C. Prado-Burguete, A. Linares-Solano, F. Rodríguez-Reinoso, C. Salinas-Martínez de Lecea, J. Catal. 115 (1989) 98–106.
[29] J. Mann, N. Yao, A.B. Bocarsly, Langmuir 22 (2006) 10432–10436.
[30] L. Jiang, H. Zang, G. Sun, Q. Xin, Chin. J. Catal. 27 (2006) 15–19.